

Isolating the ring-redox states of boron sub-phthalocyanines

Electronic Supplementary Information

Wen Zhou,^a Declan McKearney,^a Yusuke Okada,^b Nagao Kobayashi,^{b*} Daniel B. Leznoff^{a*}

^a *Department of Chemistry, Simon Fraser University, 8888 University Drive, Burnaby, BC, Canada
V5A 1S6*

^b *Faculty of Textile Science and Technology, Shinshu University, Ueda 386-8567, Japan*

* Email: nagaok@shinshu-u.ac.jp; dleznoff@sfu.ca

Experimental Section

General Materials and Methods

All techniques and procedures were carried out under a nitrogen atmosphere either with an Mbraun Labmaster 130 glovebox or using standard Schlenk and vacuum-line techniques. All glassware was dried overnight at 160 °C prior to use. Toluene, tetrahydrofuran (THF), dimethoxyethane (DME) and benzene were distilled from sodium/benzophenone under nitrogen. Hexanes were distilled from sodium under nitrogen. KC_8 was prepared from a literature procedure.¹ All other reagents were purchased from commercial sources and used without further purification. NMR spectra were recorded at 294 K, unless otherwise stated, on a 400 MHz Bruker Avance III spectrometer, a 500 MHz Bruker Avance III spectrometer, or a 600 MHz Bruker Avance II spectrometer with a 5 mm QNP cryoprobe. All ^1H NMR shifts are reported relative to the impurity of internal solvent. The ESR spectrum of **3** was collected using a Bruker EMXplus spectrometer operating at X-band (~9.3 GHz) with a PremiumX microwave bridge and HS resonator, where samples were placed in 4 mm outer-diameter quartz tubes sealed with 'O' ring needle valves. Elemental analyses (C, H, N) were performed at Simon Fraser University by Mr. Paul Mulyk on a Carlo Erba EA 1110 CHN elemental analyzer. UV-vis were recorded on a Varian Cary 5000 spectrophotometer in a 0.1 cm quartz cell or a 0.1 cm quartz cell equipped with a HI-VAC Kontes PTFE plug for air-sensitive samples.

Single Crystal X-Ray Diffraction. All crystals were mounted on a MiTeGen MicroMount using Paratone oil and measurements were made on a Bruker APEX II diffractometer with TRIUMPH-monochromated Cu $\text{K}\alpha$ radiation ($\lambda = 1.54178 \text{ \AA}$ Cu-microsource). The data were collected at a temperature of 150 K in a series of scans in 1.00° oscillations. Data were collected and integrated

using the Bruker SAINT software package² and were corrected for absorption effects using the multi-scan technique (SADABS)³ or (TWINABS).⁴ Both $(K^+ [^{sub}PcB^-])_3$ (**1**) and $[^{Sub}PcBF]SbF_6$ (**3**) crystals have poor diffraction data sets due to poor crystal quality and size. Complex $^{sub}PcBF \cdot Benzene$ (**2**) crystallized as two half molecules in the asymmetric unit cell. The structures were solved with direct methods (SIR92) and dual space methods, subsequent refinements were performed using SHELXL and ShelXle.⁵ All non-hydrogen atoms were refined anisotropically. All hydrogen atoms were placed in calculated positions but not refined. All refinements were performed using the SHELXTL crystallographic software package of Bruker-AXS.⁶ The molecular drawings were generated by the use of POV-RAY.⁷ Additional crystallographic details can be found in Table S1 and are also available from the Cambridge Crystallographic Data Centre as CCDC 2368551–2368554.

The Gaussian 16 software package was used to carry out DFT and TDDFT calculations using the CAM-B3LYP functional with 6-31+G(*d,p*) basis sets.⁸ The experimental peak corresponding to 304 nm could not be calculated due to the large molecular size of **1**.

Synthetic Procedures

$(K^+ [^{sub}PcB^-] \cdot DME_2)_3$ (**1**). To a suspension of $^{sub}PcBCl$ (86 mg, 0.20 mmol) in 10 mL THF, KC_8 (60 mg, 0.45 mmol) was added slowly, causing solubilization of the starting materials and generating a dark blue/purple solution. After being stirred for 48 h, the solvent was removed *in vacuo*, the residue was extracted with 6 mL DME / 2 mL hexanes sequentially and then the extracts were filtered through Celite. Purple-blue crystals of $(K^+ [^{sub}PcB^-] \cdot DME_2)_3$ (**1**) were isolated (57 mg, 40%) from a DME solution. UV-vis (THF): λ_{max} 460 and 750 nm; Anal. Calcd for

(C₂₄H₁₂N₆BK)₃(DME)₆: C, 62.54; H, 5.25; N, 13.68. Found C, 62.65; H, 5.18; N, 13.76. ¹H NMR (400 MHz, THF/toluene-*d*8): 5.24 (br s, 6H, ArH), and 4.27 (br s, 6H, ArH) ppm.

*sub*PcBF·Benzene (**2**). To a suspension of ^{sub}PcBCl (43 mg, 0.10 mmol) in 10 mL toluene solid AgSbF₆ (35 mg, 0.10 mmol) was added slowly. After being stirred for 20 h, the solvent was removed *in vacuo*, the residue was extracted with 4 mL benzene / 2 mL toluene sequentially, and then the extracts were filtered through Celite. Black crystals of ^{sub}PcBF·Benzene (**2**) were isolated (28 mg, 57%). UV-vis: (THF) λ_{max} 310, 561.

[*sub*PcBF][SbF₆]·Toluene (**3**). To a suspension of ^{sub}PcBCl (43 mg, 0.10 mmol) in 10 mL toluene, AgSbF₆ (75 mg, 0.22 mmol) was added slowly, causing the solution to become dark blue/purple. After being stirred for 20 h, the solvent was removed *in vacuo*, the residue was extracted with 4 mL toluene / 2 mL hexanes sequentially, and then the extracts were filtered through Celite. Black crystals of [^{sub}PcBF][SbF₆]·toluene (**3**) were isolated (20 mg, 27%). UV-vis: (THF) λ_{max} 310, 561 and 606 nm; Anal. Calcd for C₂₄H₁₂N₆BFSbF₆(C₇H₈)₂: C, 54.71; H, 3.38; N, 10.08. Found C, 54.96; H, 3.33; N, 13.24. ¹H NMR (400 MHz, toluene-*d*8): 8.67 (br s, 6H, ArH), and 7.40 (br s, 6H, ArH) ppm. ESR (THF, 77 K): *g* = 2.001.

[*sub*PcBF][SbF₆]·[Ag(DME)₃][SbF₆] (**4**). Following the same reaction as for **3** above, after the toluene extraction, the residue was extracted with 4 mL DME / 2 mL hexanes sequentially, and then the extracts were filtered through Celite. A few black crystals of ^{sub}PcBFSbF₆·Ag(DME)₃SbF₆ (**4**) were isolated (10 mg, 8%).

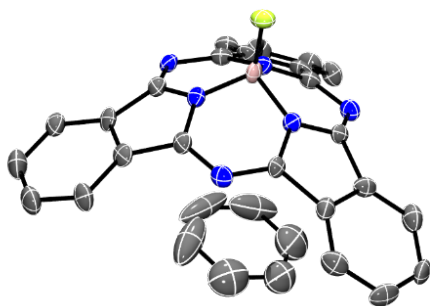


Figure S1. Solid-state molecular structure (50 % ellipsoids) of **2•benzene**. All H atoms are omitted for clarity. Colour scheme: B: light brown, F: green, N: blue and C: gray.

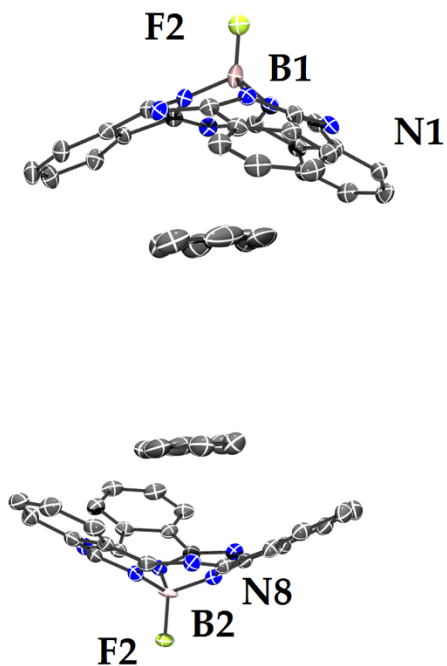


Figure S2: Concave-shaped ^{sub}PcBF units in **2** encapsulate two benzene molecules via π - π interactions.

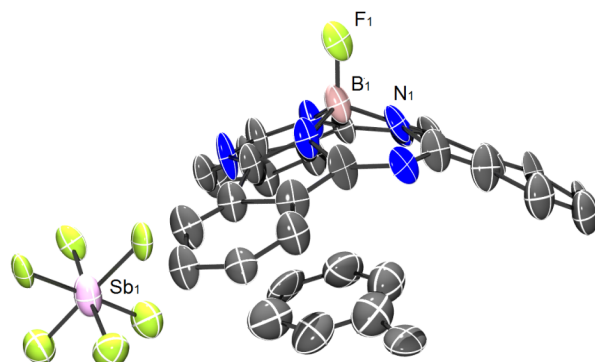


Figure S3: Solid-state molecular structure (50 % ellipsoids) of **3**. All H atoms are omitted for clarity. Colour scheme: B: light brown, Sb: pink, F: green, N: blue and C: gray

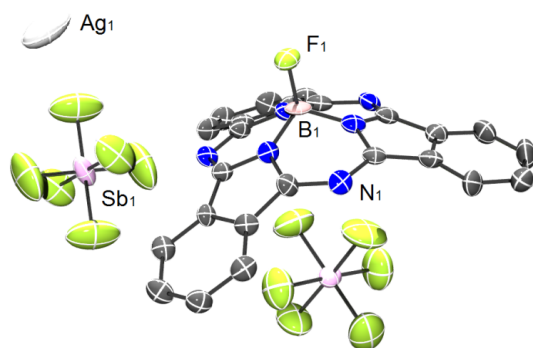


Figure S4: Solid-state molecular structure (50 % ellipsoids) of **4**. All H atoms and DME solvents are omitted for clarity. Colour scheme: Ag: light gray, B: light brown, Sb: pink, F: green, N: blue and C: gray.

Table S1. Crystallographic data for complexes 1-4.

| Compound | (K ⁺ [^{sub} PcB ⁻]) ₃ (1) | ^{sub} PcBF·Benzene (2) | [^{sub} PcBF][SbF ₆] •toluene (3) | ^{sub} PcBFSbF ₆ • Ag(DME) ₃ SbF ₆ (4) |
|--|---|---|--|--|
| Empirical formula | C ₅₂₇ H ₂₉₄ B ₁₈ K ₁₈ N ₁₀₈ O ₄₅ | C ₃₀ H ₁₈ BFN ₆ | C ₃₁ H ₂₀ BF ₇ N ₆ Sb | C ₂₆₃ H ₂₅₅ Ag ₄ B ₈ F ₈₀ N ₄₈ O ₃₂ Sb ₁₂ |
| Formula weight | 9757.06 | 492.31 | 742.09 | 8099.09 |
| Temperature/K | 150.03 | 150.15 | 150.15 | 150.15 |
| Crystal system | trigonal | monoclinic | monoclinic | monoclinic |
| Space group | P3 | P2 ₁ /m | C2/c | I2/a |
| a/Å | 27.0235(7) | 10.8237(7) | 17.0434(13) | 23.995(2) |
| b/Å | 27.0235(7) | 14.3172(10) | 15.2817(12) | 15.5710(12) |
| c/Å | 21.5015(13) | 16.0555(12) | 23.1365(19) | 26.2282(18) |
| α/° | 90 | 90 | 90 | 90 |
| β/° | 90 | 108.756(4) | 101.530(5) | 107.704(7) |
| γ/° | 120 | 90 | 90 | 90 |
| Volume/Å ³ | 13598.2(11) | 2355.9(3) | 5904.3(8) | 9335.4(13) |
| Z | 1 | 4 | 8 | 1 |
| ρ _{calc} g/cm ³ | 1.191 | 1.388 | 1.670 | 1.441 |
| μ/mm ⁻¹ | 1.836 | 0.728 | 8.111 | 9.264 |
| F(000) | 5001.0 | 1016.0 | 2936.0 | 3985.0 |
| Crystal size/mm ³ | 0.206 × 0.124 × 0.066 | 0.728 × 0.7528 × 0.6452 | 0.103 × 0.083 × 0.075 | 0.285 × 0.139 × 0.059 |
| Radiation | CuKα (λ = 1.54178) | CuKα (λ = 1.54178) | CuKα (λ = 1.54178) | CuKα (λ = 1.54178) |
| 2θ range for data collection/° | 5.582 to 139.53 | 8.484 to 133.292 | 7.8 to 124.996 | 6.688 to 137.824 |
| Index ranges | -29 ≤ h ≤ 32, -28 ≤ k ≤ 32, -25 ≤ l ≤ 22 | -12 ≤ h ≤ 12, -16 ≤ k ≤ 17, -18 ≤ l ≤ 15 | -19 ≤ h ≤ 19, -17 ≤ k ≤ 17, -26 ≤ l ≤ 26 | -28 ≤ h ≤ 28, -18 ≤ k ≤ 18, -31 ≤ l ≤ 31 |
| Reflections collected | 73113 | 21028 | 28175 | 126909 |
| Independent reflections | 27856 [R _{int} = 0.1215, R _{sigma} = 0.1417] | 4261 [R _{int} = 0.0380, R _{sigma} = 0.0349] | 4610 [R _{int} = 0.0662, R _{sigma} = 0.0457] | 8581 [R _{int} = 0.0883, R _{sigma} = 0.0269] |
| Data/restraints/parameter s | 27856/6908/29 52 | 4261/84/361 | 4610/233/501 | 8581/574/695 |
| Goodness-of-fit on F ² | 1.276 | 1.049 | 1.196 | 1.062 |
| Final R indexes [I ≥ 2σ (I)] | R ₁ = 0.1432, wR ₂ = 0.3614 | R ₁ = 0.0522, wR ₂ = 0.1418 | R ₁ = 0.1999, wR ₂ = 0.4074 | R ₁ = 0.0891, wR ₂ = 0.2540 |
| Final R indexes [all data] | R ₁ = 0.2500, wR ₂ = 0.4416 | R ₁ = 0.0576, wR ₂ = 0.1465 | R ₁ = 0.2201, wR ₂ = 0.4146 | R ₁ = 0.0916, wR ₂ = 0.2577 |
| Largest diff. peak/hole / e Å ⁻³ | 1.06/-0.76 | 1.04/-0.46 | 1.66/-2.97 | 2.29/-2.26 |

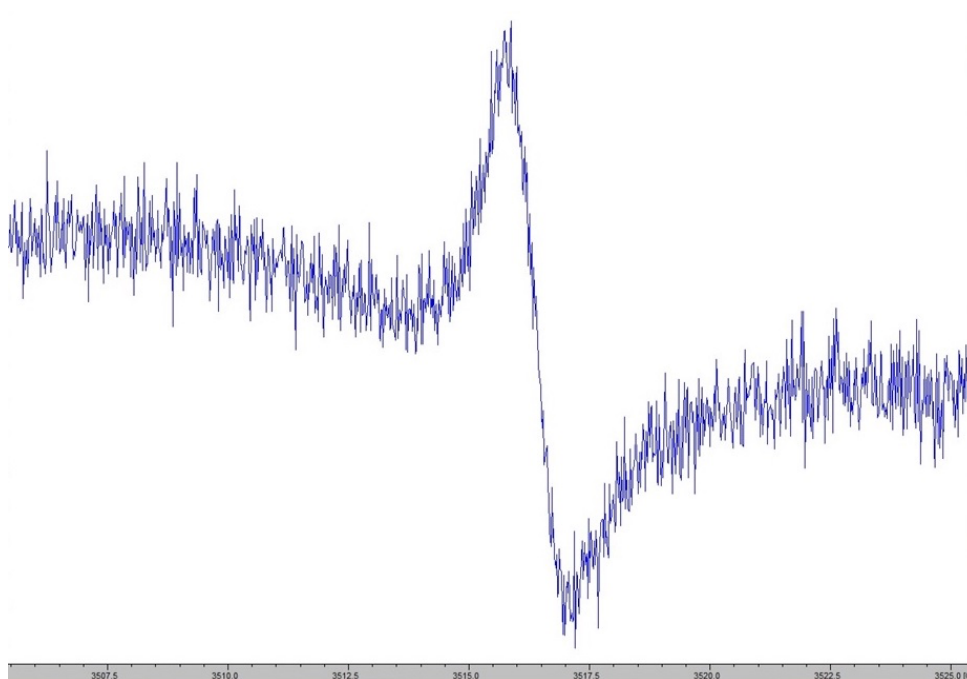


Figure S5: ESR spectrum of **3** in toluene solution at room temperature.

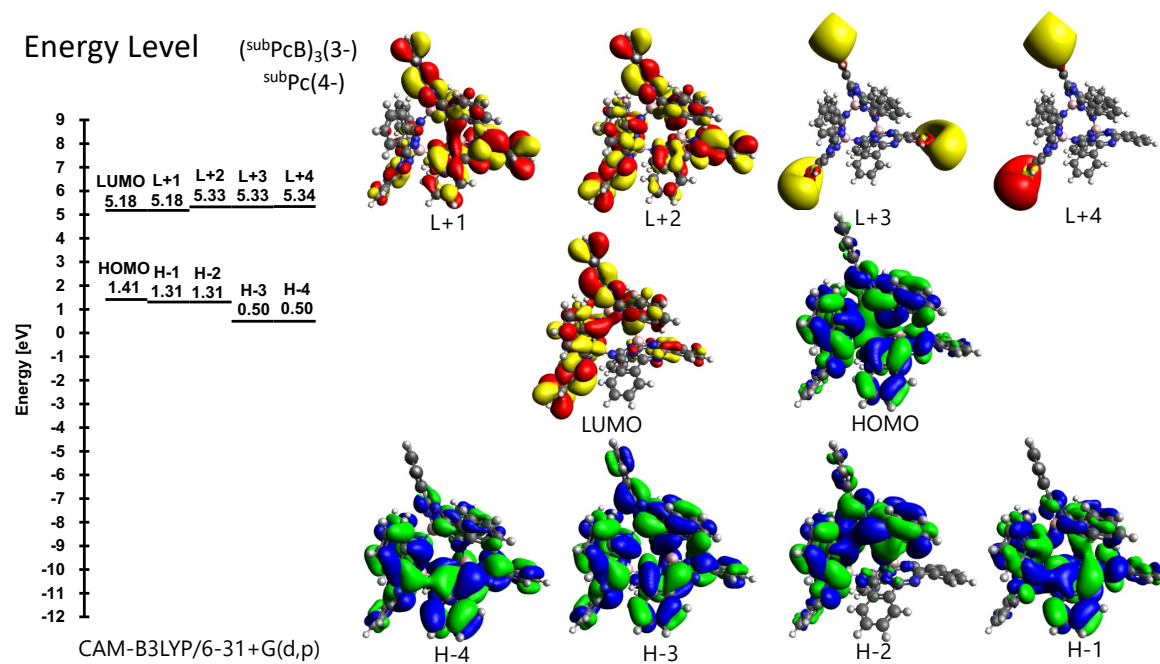


Figure S6. Energies and shapes of selected key frontier orbitals of **1**.

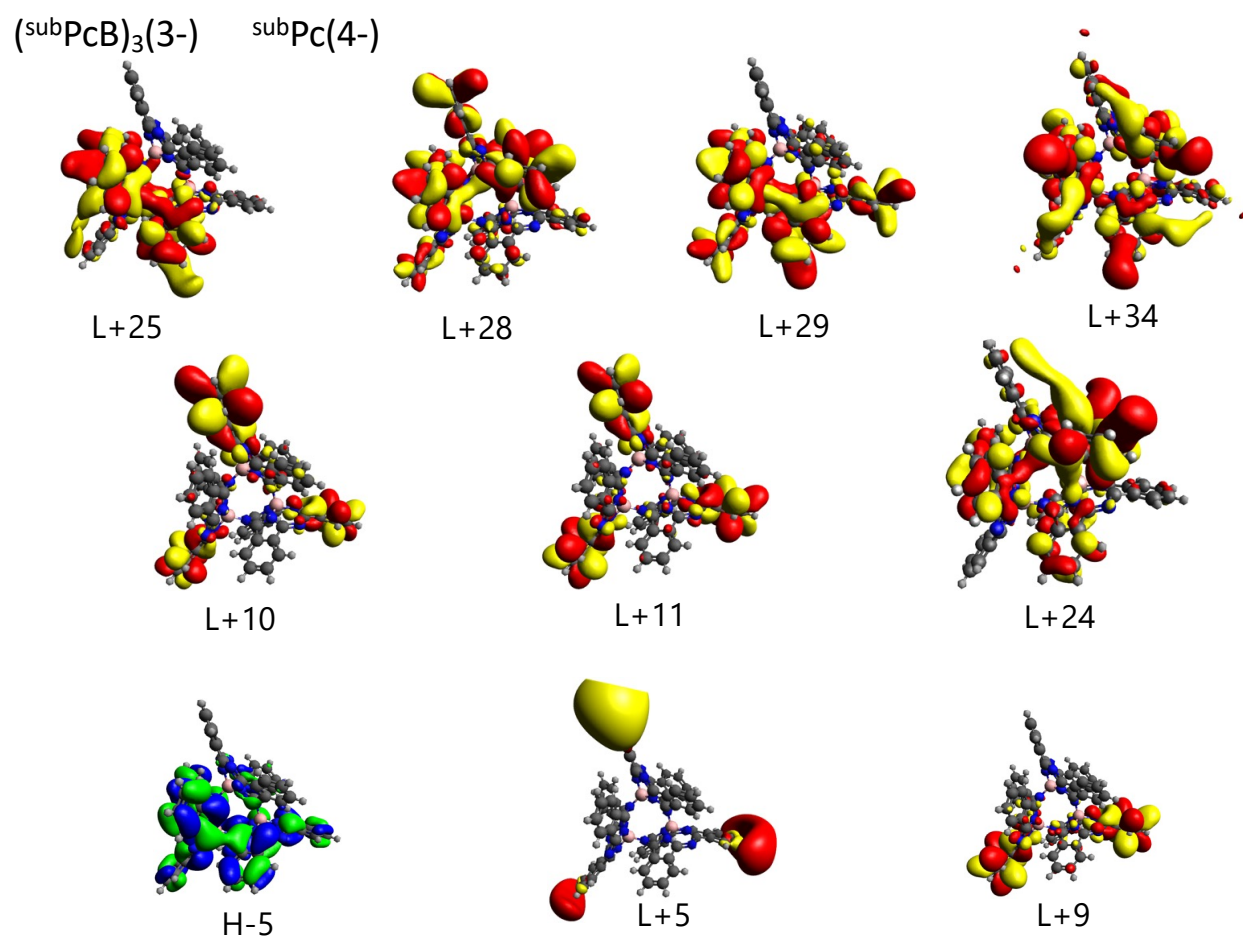


Figure S7. Shapes of selected additional frontier orbitals of **1**.

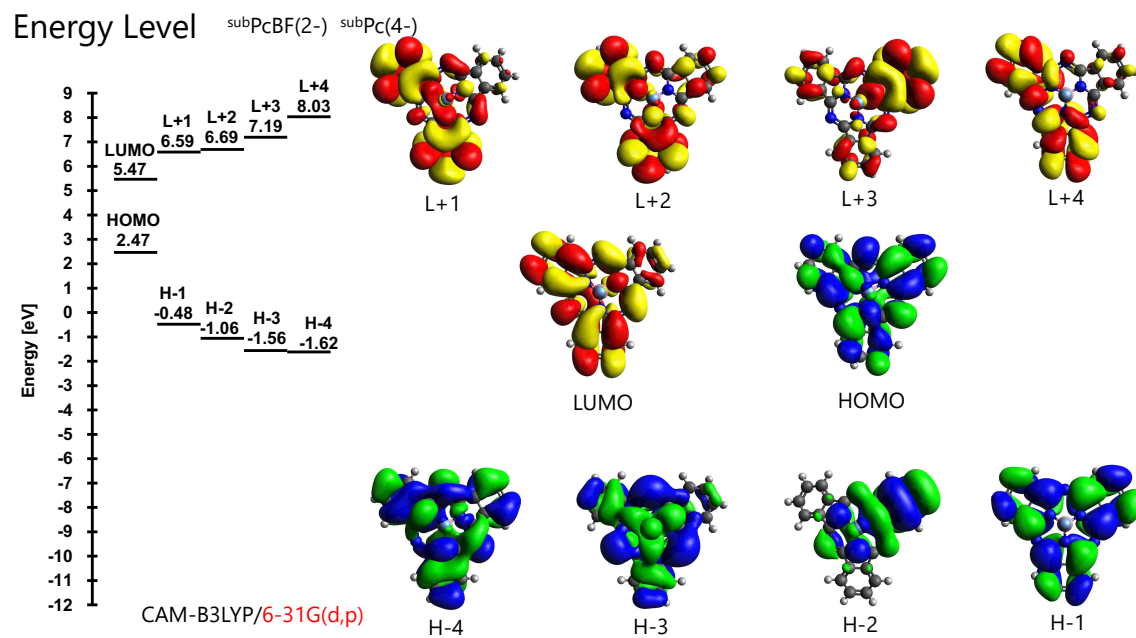


Figure S8. Energies and shapes of selected key frontier orbitals for the putative mononuclear $[\text{SubPcB}]^{2-}$ unit where the ring-oxidation state is $\text{SubPc}(4-)$.

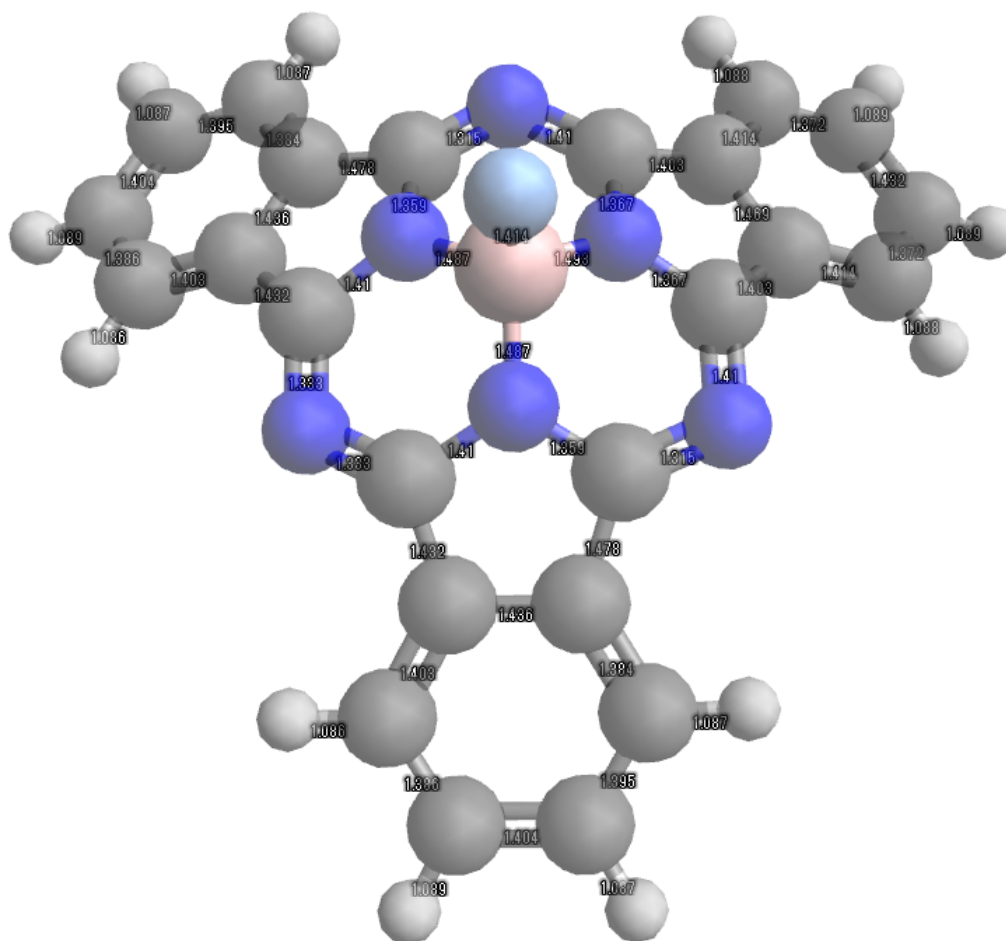


Figure S9. Calculated bond lengths for the putative mononuclear $[\text{SubPcB}]^{2-}$ unit where the ring-oxidation state is $\text{SubPc}(4-)$

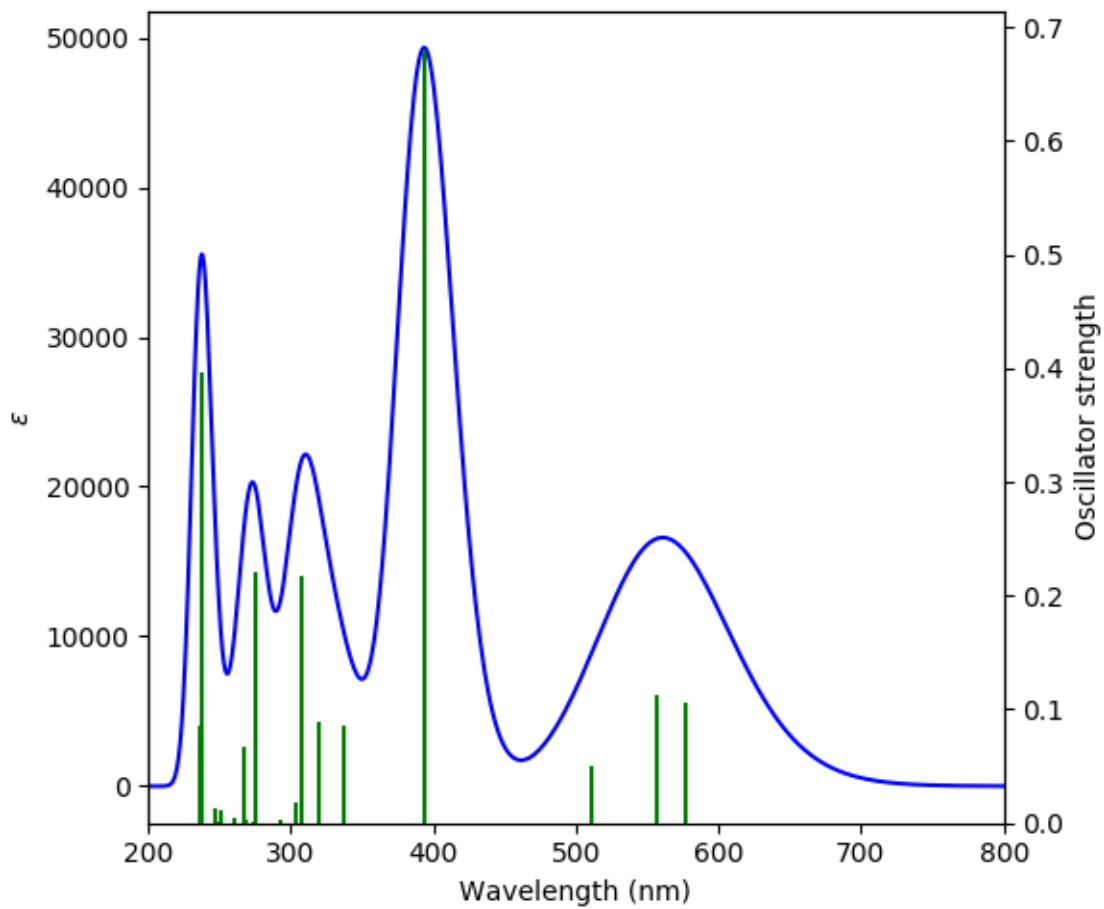


Figure S10. TD-DFT Calculated absorption spectrum for the putative mononuclear $[\text{SubPcB}]^{2-}$, where ring-oxidation state is $\text{SubPc}(4-)$

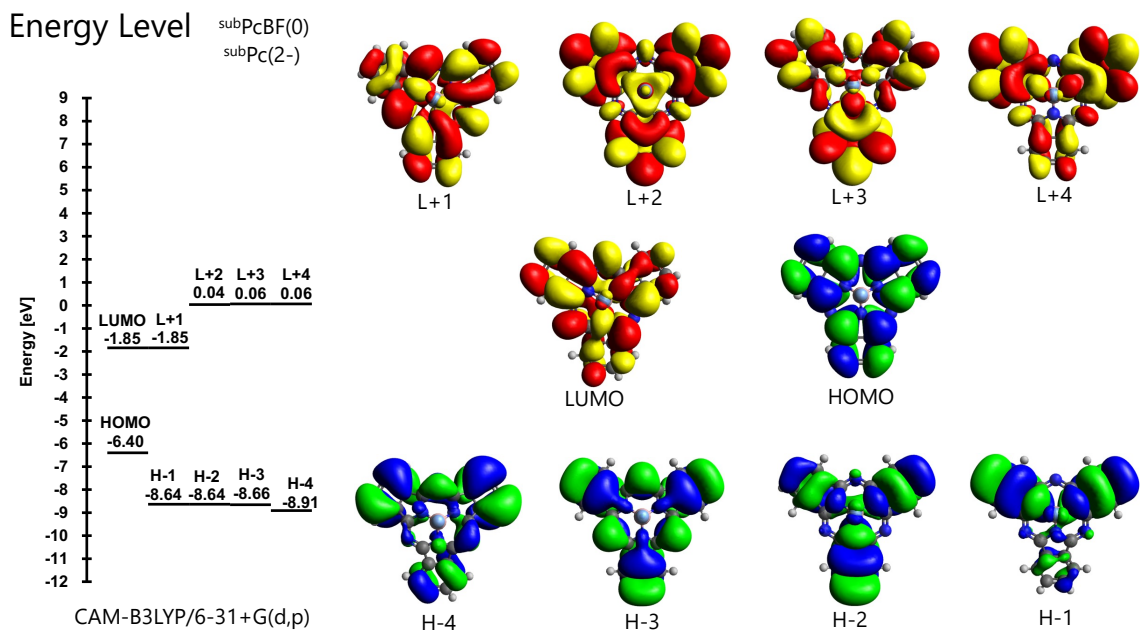


Figure S11. Energies and shapes of selected key frontier orbitals of **2**.

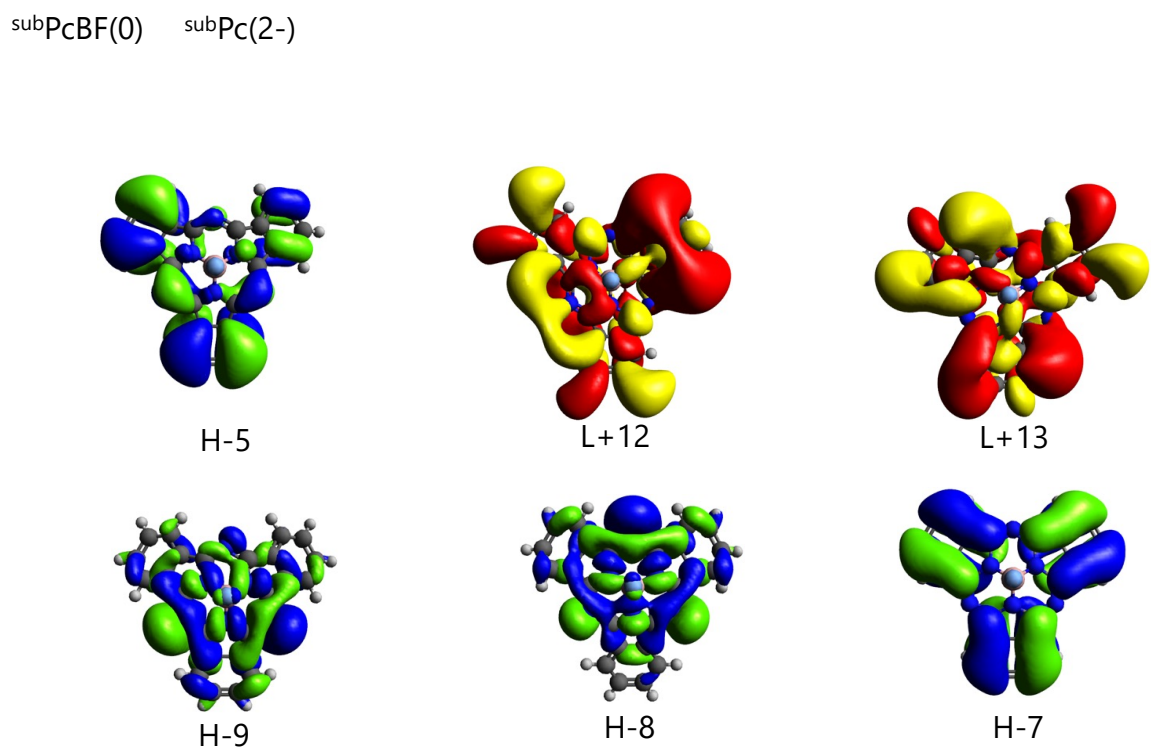


Figure S12. Shapes of selected additional frontier orbitals of **2**.

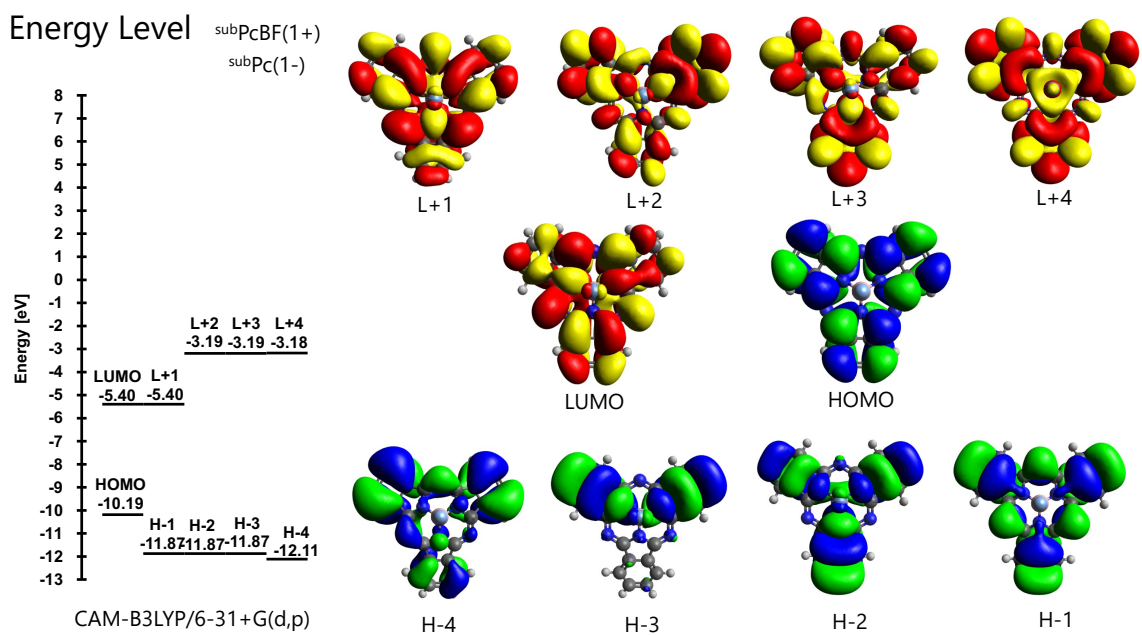


Figure S13. Energies and shapes of selected key frontier orbitals of **3**.

subPcBF(1+) subPc(1-)

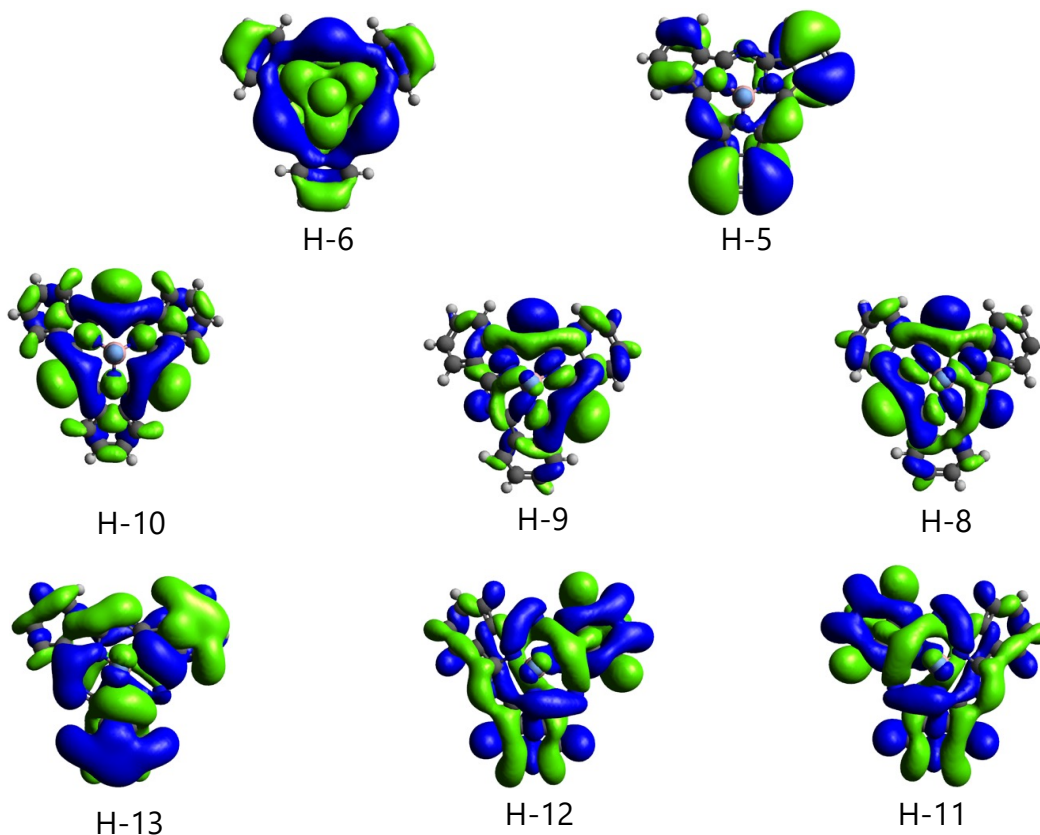


Figure S14. Shapes of selected additional frontier orbitals of **3**.

Table S2. Calculated transition energies, oscillator strength (f), and compositions of cyclic SubPc trimer **1**.^a

| Energy/eV (nm) | f | Compositions (%) |
|----------------|--------|--|
| 1.80 (690.6) | 0.1972 | H-2→L(29), H-1→L+1(29), H→L+2(23) |
| 2.35 (528.4) | 0.0208 | H→L+2(34), H-2→L+1(32), H-1→L(32) |
| 2.75 (450.3) | 0.0310 | H→L+10(18), H-3→L+1(16), H-1→L+11(12), H-4→L+2(10) |
| 2.75 (450.3) | 0.0311 | H→L+9(18), H-3→L(15), H-2→L+11(12), H-5→L+2(10) |
| 2.94 (422.1) | 0.5624 | H→L+10(22), H-1→L+11(14), H-3→L+1(13) |
| 2.94 (422.1) | 0.5625 | H→L+9(22), H-2→L+11(14), H-3→L(13) |
| 3.03 (408.6) | 0.1786 | H-1→L+3(18), H→L+4(13) |

| | | |
|--------------|--------|--|
| 3.03 (408.6) | 0.1786 | H-2→L+3(18), H→L+5(13) |
| 3.08 (402.1) | 0.2314 | H→L+24(15) |
| 3.08 (402.1) | 0.2313 | H→L+25(15) |
| 3.21 (386.3) | 0.0302 | H-1→L+11(22), H→L+9(20) |
| 3.21 (386.3) | 0.0302 | H-2→L+11(22), H→L+10(20) |
| 3.22 (385.3) | 0.1310 | H-2→L+29(19), H-1→L+28(17), H→L+34(14) |

^aTransitions with f greater than 0.02 and compositions larger than 10% are collected.

Table S3. Calculated transition energies, oscillator strength (f), and compositions of the putative mononuclear [^{Sub}PcB]²⁻, where ring-oxidation state is ^{Sub}Pc(4-).^a

| No. | Energy [eV] | Wavelength [nm] | f | Major contribs |
|-----|-------------|-----------------|--------|---|
| 1 | 0.77 | 1616.9 | 0.0362 | HOMO→LUMO (93%) |
| 2 | 2.15 | 576.3 | 0.1053 | HOMO→L+1 (92%) |
| 3 | 2.23 | 557.1 | 0.1121 | HOMO→L+2 (97%) |
| 4 | 2.43 | 510.8 | 0.0495 | HOMO→L+3 (92%) |
| 5 | 3.15 | 393.6 | 0.6805 | H-1→LUMO (95%) |
| 6 | 3.68 | 336.5 | 0.0852 | HOMO→L+4 (96%) |
| 7 | 3.88 | 319.4 | 0.0884 | HOMO→L+6 (79%) |
| 8 | 4.04 | 306.9 | 0.2167 | H-1→L+2 (27%), HOMO→L+5 (55%) |
| 9 | 4.09 | 303.5 | 0.0177 | H-1→L+1 (82%) |
| 10 | 4.24 | 292.7 | 0.0033 | H-1→L+2 (67%), HOMO→L+5 (26%) |
| 11 | 4.52 | 274.6 | 0.2199 | H-7→LUMO (10%), H-6→LUMO (16%), H-3→LUMO (31%), H-2→LUMO (29%) |

| | | | | |
|----|------|-------|--------|--|
| 12 | 4.53 | 273.6 | 0.0006 | H-4->LUMO (77%) |
| 13 | 4.62 | 268.4 | 0.0037 | H-1->L+3 (80%) |
| 14 | 4.64 | 267.1 | 0.0667 | H-6->LUMO (28%), H-3->LUMO (10%), H-2->LUMO (46%) |
| 15 | 4.76 | 260.3 | 0.0051 | H-5->LUMO (81%) |
| 16 | 4.94 | 251.1 | 0.0106 | H-6->LUMO (32%), H-3->LUMO (32%), HOMO->L+8 (13%), HOMO->L+10 (10%) |
| 17 | 4.96 | 250.0 | 0.0008 | HOMO->L+7 (91%) |
| 18 | 5.03 | 246.3 | 0.0131 | HOMO->L+8 (80%) |
| 19 | 5.22 | 237.6 | 0.3968 | H-7->LUMO (45%), H-5->L+2 (10%) |
| 20 | 5.24 | 236.7 | 0.0850 | H-9->LUMO (25%), H-2->L+3 (11%), H-1->L+4 (13%) |

^aTransitions with f greater than 0.02 and compositions larger than 10% are collected.

Table S4. Calculated transition energies, oscillator strength (f), and compositions of neutral ^{Sub}Pc(2-)BF **2** and mono-cationic [^{Sub}Pc(1-)BF]⁺ **3**. ^a

| Energy/eV (nm) | f | Compositions (%) |
|---|--------|---|
| Neutral ^{Sub} Pc(2-)BF, 2 | | |
| 2.56 (483.7) | 0.3719 | H→L(93) |
| 2.56 (483.7) | 0.3719 | H→L+1(93) |
| 4.25 (292.0) | 0.0256 | H→L+3(31), H-1→L+1(15), H-2→L(15), H-1→L(11), H-2→L+1(11) |
| 4.25 (292.0) | 0.0256 | H→L+4(31), H-1→L(15), H-2→L+1 (15), H-1→L+1(11), H-2→L(11) |
| 4.74 (261.4) | 0.1345 | H-3→L(23), H-9→L+1(13), H-8→L(12), H-4→L(11), H-5→L+1(11) |
| 4.74 (261.4) | 0.1345 | H-3→L+1(23), H-8→L+1(13), H-9→L(12), H-4→L+1(11), H-5→L(11) |
| 4.82 (257.3) | 0.7840 | H-3→L+1(36), H-1→L(12) |
| 4.82 (257.3) | 0.7841 | H-3→L(36), H-3→L+1(12) |
| 4.93 (251.3) | 0.0460 | H-2→L(21), H-1→L+1(21) |
| 5.52 (224.5) | 0.0354 | H-7→L(32) |
| 5.52 (224.5) | 0.0354 | H-7→L+1(32) |
| 6.09 (203.6) | 0.4425 | H→L+12(29), H-2→L+2(11) |
| 6.09 (203.6) | 0.4425 | H→L+13(29), H-1→L+2(11) |

Mono-cationic [^{Sub}Pc(1-)BF]⁺, **3**

| | | |
|--------------|--------|---|
| 2.07 (599.4) | 0.0620 | H(a)→L(a)(82) |
| 2.07 (599.4) | 0.0520 | H(a)→L+1(a)(82) |
| 2.69 (461.0) | 0.2175 | H(b)→L(b)(62),H-2(b)→L(b)(12) |
| 2.69 (461.0) | 0.2175 | H-1(b)→L(b)(62),H-3(b)→L(b)(12) |
| 3.48 (356.2) | 0.0363 | H-1(a)→L+1(a)(16), H-2(a)→L+1(a)(11), H-3(a)→L(a)(11) |
| 3.48 (356.2) | 0.0363 | H-1(a)→L(a)(16), H-2(a)→L(a)(11), H-3(a)→L+1(a)(11) |
| 3.87 (320.5) | 0.0254 | H-1(a)→L(a)(30), H-6(a)→L(a)(11) |
| 3.87 (320.5) | 0.0254 | H-1(a)→L+1(a)(30), H-6(a)→L+1(a)(11) |
| 4.02 (308.3) | 0.0326 | H-3(a)→L(a)(20), H-2(a)→L+1(a)(20), H(a)→L+2(a)(12) |
| 4.02 (308.3) | 0.0326 | H-3(a)→L+1(a)(20), H-2(a)→L(a)(20), H(a)→L+3(a)(12) |
| 4.25 (291.5) | 0.0527 | H-6(a)→L(a)(39) |
| 4.25 (291.5) | 0.0527 | H-6(a)→L+1(a)(39) |
| 4.32 (286.8) | 0.1177 | H-1(a)→L(a)(12) |
| 4.32 (286.8) | 0.1177 | H-1(a)→L+1(a)(12) |
| 4.48 (276.7) | 0.0361 | H-9(a)→L+1(a)(21), H-8(a)→L(a)(21) |
| 4.48 (276.7) | 0.0361 | H-9(a)→L(a)(21), H-8(a)→L+1(a)(21) |
| 4.79 (259.0) | 0.1492 | H-10(b)→L(b)(24) |
| 4.79 (259.0) | 0.1492 | H-11(b)→L (b)(24) |
| 4.85 (255.4) | 0.0884 | H-4(b)→L+2(b)(19) |
| 4.85 (255.4) | 0.0884 | H-4(b)→L+1(b)(19) |
| 4.93 (251.3) | 0.1630 | H(a)→L+2(a)(11), H-1(b)→L+1(b)(11),H(b)→L+2(b)(11) |
| 4.93 (251.3) | 0.1630 | H(a)→L+3(a)(11), H-1(b)→L+2(b)(11),H(b)→L+1(b)(11) |
| 5.21 (237.8) | 0.0803 | H-13(b)→L(b)(24) |
| 5.21 (237.8) | 0.0803 | H-12(b)→L(b)(24) |
| 5.28 (234.7) | 0.0361 | H-3(b)→L+1(b)(22),H-2(b)→L+2(b)(22) |
| 5.31 (233.4) | 0.1588 | H-4(b)→L+1(b)(20) |
| 5.31 (233.4) | 0.1588 | H-4(b)→L+2(b)(20) |
| 5.43 (228.5) | 0.0451 | H-5(b)→L+2(b)(20),H-12(b)→L(b)(13) |
| 5.43 (228.5) | 0.0451 | H-5(b)→L+1(b)(20),H-13(b)→L(b)(13) |

^aTransitions with *f* greater than 0.02 and compositions larger than 10% are collected.

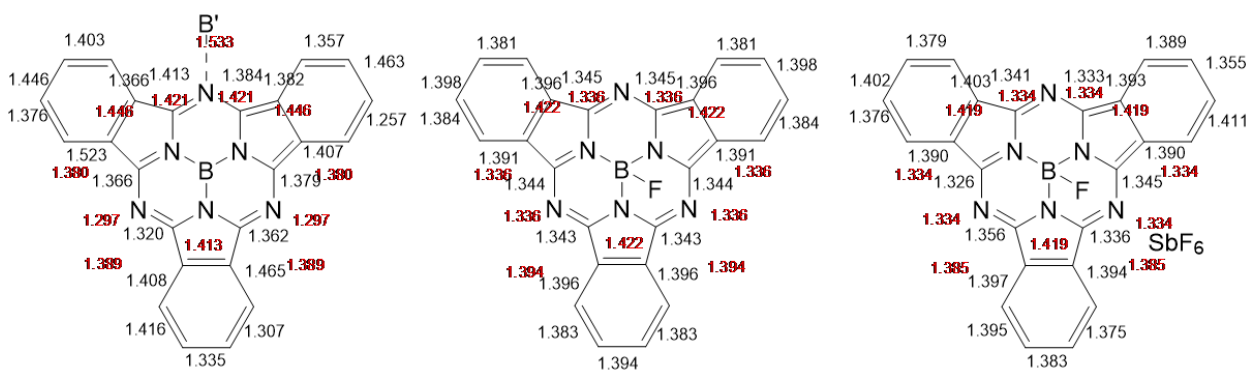


Figure S15: From left to right, metrical parameters for doubly ring-reduced $\text{subPc}(4-)$ in $(\text{K}^+[\text{subPcB}^-])_3$ (**1**), standard $\text{subPc}(2-)$ in subPcBF (**2**) and ring-oxidized $\text{subPc}(1-)$ in $[\text{subPcBF}][\text{SbF}_6] \cdot \text{Ag}(\text{DME})_3\text{SbF}_6$ (**4**). The red numbers are calculated bond lengths from the DFT optimized structures.

References

- [1] MA Schwindt, T Lejon, LS Hegedus, *Organometallics*, **1990**, *8*, 2814-2819.
- [2] SAINT, version 7.46A; Bruker Analytical X-ray System: Madison, WI, 1997-2007.
- [3] SADABS. Bruker Nonius area detector scaling and absorption correction, V2.10; Bruker AXS Inc.: Madison, WI, 2003.
- [4] (a) TWINABS, Bruker Nonius scaling and absorption for twinned crystals, V2008/2; Bruker AXS Inc.: Madison WI, 2008. (b) TWINABS, Bruker Nonius scaling and absorption for twinned crystals, V1.05; Bruker AXS Inc.: Madison, WI, 2007.
- [5] (a) G. M. Sheldrick, *Acta Crystallogr. Sect. C Struct. Chem.* **2015**, *71*, 3-8.
(b) C. B. Hübschle, G. M. Sheldrick, B. Dittrich, *J. Appl. Crystallogr.* **2011**, *44*, 1281-1284.
- [6] (a) SHELXTL, Version 5.1; Bruker AXS Inc.: Madison, WI, 1997. (b) T. D. Fenn, D. Ringe, G. A. Petsko, *J. Appl. Crystallogr.* **2003**, *36*, 944-947.
- [7] L. J. Farrugia, *J. Appl. Crystallogr.* **1997**, *32*, 565.
- [8] M. J. Frisch *et al.* *Gaussian 16, Revision A.03*; Gaussian, Inc.: Wallingford, CT, 2016.